Available online at www.sciencedirect.com
SCIENCE DIRECT®
Bioorganic & Medicinal Chemistry 13 (2005) 809–817
Bioorganic & Medicinal Chemistry

Design, synthesis and photobiological properties of 3,4-cyclopentenepsoralens

Ornella Gia,[a] Sebastiano Marciani Magno,[a] Humberto Gonzalez-Diaz,[b] Elias Quezada,[b] Lourdes Santana,[b] Eugenio Uriarte[b] and Lisa Dalla Via[a,*]

[a]*Department of Pharmaceutical Sciences, University of Padova, via Marzolo, 5, 35131 Padova, Italy*
[b]*Department of Organic Chemistry, University of Santiago de Compostela, Santiago de Compostela, 15706, Spain*

Received 6 July 2004; accepted 18 October 2004
Available online 11 November 2004

Abstract—The QSAR directed synthesis of tetracyclic psoralen derivatives (**3**–**5**) characterised by the condensation of a cyclopentane ring at the level of the 3,4 double bond of the tricyclic psoralen moiety is reported. The new compounds present a methoxy (**3**), a hydroxy (**4**) or a dimethylaminopropoxy (**5**) side chain inserted in position 8 of the lead chromophore. The evaluation of photoantiproliferative activity on human tumour cell lines reveals for **5** an ability to inhibit cell growth significantly higher with respect to that of the reference drug, 8-MOP. Interestingly, the enhancement in antiproliferative activity is accompanied by the disappearance of skin phototoxicity. On the other hand, no significant photobiological activity was scored for **3** and **4**. The ability to photoreact with DNA, evaluated by isolating the 4′,5′ monoadduct and by estimating the ability to form interstrand cross-links, appeared to be significant for **5**, practically negligible for **3** and **4**. Furthermore, a back-projection of the more active compound identifies structural features suitable for further synthetic modifications.

1. Introduction

Nowadays, the employment of psoralen derivatives in PUVA (Psoralen plus UVA) therapy is well-established for both skin hyperproliferative diseases (such as psoriasis) and cutaneous T-cell lymphoma.[1–4] In particular, 8-methoxypsoralen (8-MOP) represents the most widely used drug, to a lesser extent its congeners 5-methoxypsoralen[5] and 4,5′,8-trimethylpsoralen.[1] Nevertheless, notwithstanding its wide employment in photochemotherapeutic treatments, the PUVA therapy suffers from important drawbacks. In particular, erythema and hyperpigmentation constitute the most common short-term side effects. Moreover, the five most likely potential long-term risks were identified: nonmelanoma skin cancer (particularly squamous cell carcinoma), melanoma, accelerated skin ageing, cataracts and increased risk of noncutaneous malignancy.[6,7]

The molecular mechanism accountable for the photobiological effects involves mainly the ability of the psoralen moiety to interact with DNA. In particular, the UVA irradiation (365 nm) of the intercalative complex to which the planar tricyclic chromophore gives rise with the macromolecule, induces the formation of covalent photomonoadducts with pyrimidine bases, mainly thymine. The ability to form diadducts, which results from the involvement of both photoreactive double bonds, that is, the 4′,5′ furan side and the 3,4 pyrone side, has already been demonstrated.[8]

To date, many studies have been devoted to the synthesis and the study of the photobiological properties of psoralen derivatives with the aim of obtaining drugs able to exert a photoantiproliferative activity comparable or higher than that of 8-MOP and to weaken the undesired side effects of the PUVA therapy. In this connection, tetracyclic analogues obtained by the condensation of a fourth ring like benzene, cyclohexane or cyclopentane, at the level of the 4′,5′ or 3,4 double bond entails interesting photobiological properties.[9–12] In particular, studies have been made of synthesised benzo and tetrahydrobenzo-psoralen derivatives characterised by the insertion of a methoxy, a hydroxy or a dimethylaminopropoxy side chain in 8- or 5-position of the lead tricyclic chromophore. Interestingly, it appeared clearly that the presence of the basic protonable side chain,

Keywords: Cyclopentenepsoralens; Synthesis; Photobiological activity; QSAR.
* Corresponding author. Tel.: +39 049 8275712; fax: +39 049 8275366; e-mail: lisa.dallavia@unipd.it

0968-0896/$ - see front matter © 2004 Elsevier Ltd. All rights reserved.
doi:10.1016/j.bmc.2004.10.044

inserted with a view to increase their low solubility in aqueous media, induced an antiproliferative activity on human tumour cell lines notably higher with respect to that of 8-MOP and a significant decrease in skin phototoxicity in comparison with the drug.[9,10] As regards compounds with a cyclopentane fused to the psoralen moiety, cyclopentenepsoralen derivatives carrying methyl groups in different positions of the tricyclic chromophore have been synthesised and photobiological studies of them reported. In general, these tetracyclic derivatives exerted a certain increase in antiproliferative ability and a slight decrease in erythema induction with respect to the reference drug, 8-MOP.[11,12]

On the basis of these previous studies, it appeared of interest to exploit a quantitative–structure–activity–relationships (QSAR) method using simple molecular descriptors to develop new psoralen derivatives. QSAR techniques are based on the use of the so-called molecular descriptors, which are numerical series codifying helpful chemical information, correlated statistically with biological properties.[13] There are many examples of successful application of these indices in lead compound discovery.[14]

In this paper the QSAR directed synthesis of cyclopentenepsoralen derivatives characterised by the condensation of the fourth ring at the level of 3,4 pyrone side double bond and carrying a methoxy (**3**), a hydroxy (**4**) or a dimethylaminopropoxy (**5**) side chain in the 8-position of the lead chromophore is reported. The ability to induce photoantiproliferative activity on human tumour cell lines was assayed along with the evaluation of appearance of erythema on guinea pig skin. The molecular mechanism of action was investigated by means of the study of the interaction with DNA in the ground state and the evaluation of the ability to photoreact with the double helix. Furthermore, the isolation and the characterisation of the furan side photoadduct between **5** and thymine was described. Finally, to gain further insight into the role played by the different molecular features of **5** a back-projection approach was applied. Specifically, the use of back-projectable approaches enables the variables on the QSAR to be projected back into the molecular space, providing for biological and chemically significant conclusions.[15] Our research group have recently introduced novel back-projectable molecular descriptors based on a simple stochastic approach known as MARCH-INSIDE (*Mar*kovian *Ch*emicals *In Si*lico *De*sign),[16] for the discovery of active compounds from structurally heterogeneous series.[17–19] Specifically, a model developed for the discovery of anticancer compounds was used in the present work.[20]

2. Results and discussion

2.1. 'In silico' evaluation

The ${}^{SR}\pi_k$ values for many compounds and Eq. 1 described in Section 4, were used to calculate the probability of psoralen derivatives **3**–**5** acting as anticancer compounds. In Table 1 the theoretical results obtained from the in silico screening are reported. As a matter of comparison, the photochemotherapeutic drug 8-MOP, which is predicted by the model with a posterior probability of 0.76, is also indicated.

Table 1. Results of the in silico screenings

Compound	$P(+)$[a]	$P(-)$[b]
3	0.35	**0.65**
4	0.45	**0.55**
5	**0.85**	0.15
8-MOP	**0.76**	0.24

[a] Posterior probability (%) by which the model classifies a chemical as anticancer (+).
[b] Posterior probability (%) by which the model classifies a chemical as nonanticancer (−).

From the values shown in Table 1 it is possible to note that the highest percentage of posterior probability to be an anticancer compound was predicted for derivative **5**: this percentage appears to be actually greater than that calculated for the reference drug. Otherwise, for both **3** and **4** the theoretical values indicate a low posterior probability, which suggests they may be predicted to be inactive derivatives.

2.2. Chemistry

The compounds studied were prepared as shown in Scheme 1. The coumarin **1** was synthesised in 91% yield by treatment of 2-methoxyresorcinol with ethyl 2-oxocyclopentanecarboxylate involving a Pechmann condensation. The synthesis of the furan ring was performed by reaction of the hydroxycoumarin **1** and chloroacetone in the presence of potassium carbonate, followed by treatment of the corresponding acetonyl derivative **2** in alkaline solution and acidification to obtain the final psoralen derivative **3** in 64% overall yield. The 8-methoxypsoralen **3** was transformed to the hydroxypsoralen **4** in 87% yield by hydrolysis of the methoxy group to hydroxyl group with aluminium chloride in methylene chloride. Treatment of compound **4** with 3-chloro-*N*,*N*-dimethylpropylamine and NaH in the presence of NaI in refluxing dimethylformamide afforded compound **5** in 64% yield.

2.3. Antiproliferative activity

The antiproliferative activity of the new cyclopentenepsoralens **3**–**5** was evaluated by means of a growth inhibition assay on two human tumour cell lines, HeLa (cervix adenocarcinoma cells) and HL-60 (promyelocytic leukaemic cells) and expressed as IC_{50} values, that is, the concentration of compound able to induce 50% of cell death with respect to the control culture. The well known photochemotherapeutic drug 8-MOP was taken as reference compound and the results are reported in Table 2.

After exposure to UVA light (365 nm) the new derivative characterised by having a dimethylaminopropoxy side chain in position 8 of the psoralen chromophore (com-

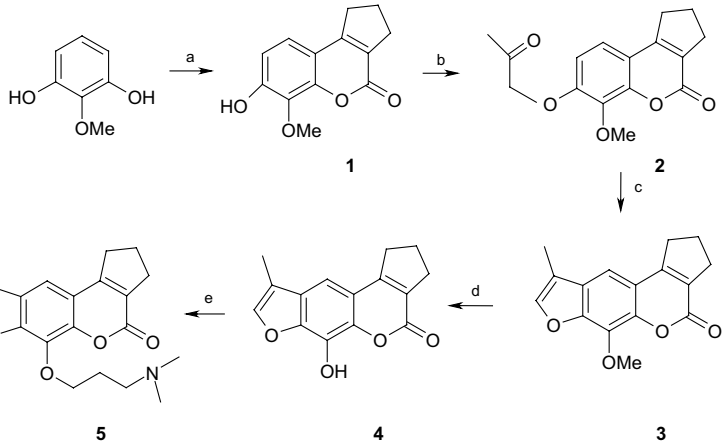

Scheme 1. Reagents and conditions: (a) ethyl 2-oxo-cyclopentanecarboxylate, H_2SO_4, rt, 91%; (b) 2-chloroacetone, K_2CO_3, Me_2CO, reflux, 77%; (c) NaOH, reflux, 83%; (d) $AlCl_3$, CH_2Cl_2, rt, 87%; (e) 3-chloro-*N*,*N*-dimethylpropylamine, NaH, NaI, DMF, 100 °C, 64%.

Table 2. Cell growth inhibition and skin phototoxicity in guinea pigs in the presence of examined compounds and 8-MOP as reference drug

Compound	IC_{50} (μM) of cell lines				Skin phototoxicity	
	HeLa		HL-60		Dose (μmol cm^{-2})	Erythema intensity[b]
	Dark	UVA	Dark	UVA		
3	>20	>20	>20	>20	0.18	—
4	>20	>20	>20	>20	0.19	—
5	18.4 ± 1.9	0.58 ± 0.13	7.7 ± 0.5	0.91 ± 0.01	0.15	—
8-MOP[a]	>20	10 ± 3	>20	5.4 ± 0.7	0.05	+ (With edema)

[a] Taken from Ref. 10.
[b] +, Strong; –, absent.

pound **5**) appears to be able to exert a noticeable capacity to inhibit cell growth. Indeed, the ability of **5** to induce the photoantiproliferative effect is significantly higher with respect to that of the reference drug. In particular, the IC_{50} value obtained for HL-60 cells is about five times lower with respect to that of 8-MOP, whilst for HeLa cells a value even 17 times lower is attained. Otherwise, the new derivatives carrying a methoxy (compound **3**) or a hydroxy (compound **4**) group in 8-position appear to be unable to exert any photoantiproliferative effect on both cell lines taken into account.

Furthermore, experiments performed in the dark confirmed both **3** and **4** to be inactive, whilst in this experimental condition a certain activity was scored for compound **5**. Nevertheless, it appears clearly that this antiproliferative ability is significantly lower compared to that exerted in the presence of UVA irradiation.

2.4. Skin phototoxicity

The evaluation of the skin phototoxicity, determined by appearance of erythema in guinea pigs, in the case of **5** revealed some interesting photobiological behaviour (Table 2): besides the capacity to exert a noticeable antiproliferative effect, the new cyclopentenepsoralen carrying the dimethylaminopropoxy side chain appears devoid of photosensitising capacity, even if applied at a concentration up to three times higher with respect to that at which the reference drug provokes a serious phototoxic effect. As regards the two cyclopentenepsoralen derivatives **3** and **4**, no appearance of any skin effect was noted.

2.5. Noncovalent binding with DNA

The planar tricyclic chromophore of the psoralen moiety undergoes intercalation between two DNA base pairs. The molecular complex that is formed with the macromolecule in the ground state is determinant for the subsequent covalent photoaddition after UVA irradiation and thus for exerting the cellular photobiological consequences.

The condensation of a further ring to the psoralen chromophore along with the insertion of a basic side chain protonable at physiological pH can be determinant for the ability of the overall tetracyclic molecule to give rise to an effective molecular complex of intercalation.[9,10] Furthermore, in a previous study theoretical calculations performed on psoralen analogues bearing a cyclopentane ring condensed to either the 4′,5′ or 3,4 double bond of the parent tricyclic chromophore, indicates that these tetracyclic moieties are practically planar.[11] On the basis of these assumptions it appears of interest to investigate the capacity of the new cyclopentenepsoralens **3**–**5** to interact with DNA in the ground state. For this purpose flow linear dichroism (LD) experiments were performed at different [drug]/[DNA] ratios. In Figure 1 the spectra of DNA solutions in the presence of

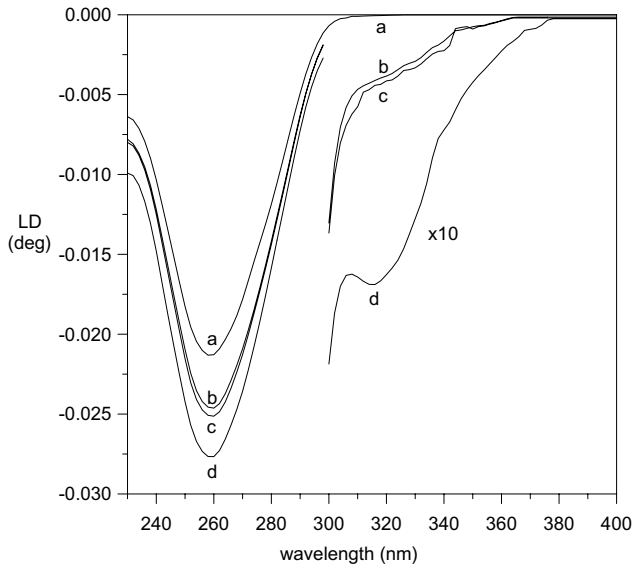

Figure 1. Linear flow dichroism spectra for salmon testes DNA alone (a) and in the presence of compounds **3** (b), **4** (c) and **5** (d) at [drug]/[DNA] ratio = 0.08. [DNA] = 1.5×10^{-3} M.

compounds **3**–**5** at [drug]/[DNA] = 0.08 are shown as representative examples. In particular, DNA spectrum (trace a) shows the typical negative LD band at 260 nm while in the presence of **5** (trace d) a significant negative signal occurs in the spectral region between 300–380 nm, where only the added drug exhibits absorption. The appearance of a dichroic signal at wavelengths higher than 260 nm indicates that the small molecule of the drug becomes oriented in the flow field as a result of the occurrence of a molecular complex with DNA. Furthermore, the negative sign of this signal is linked to an orientation of the molecular plane of the cyclopentenepsoralen chromophore parallel to the plane of DNA bases thus indicating for compound **5** the ability to give rise to an intercalative mode of binding with the macromolecule.

As regards compounds **3** and **4**, the spectra of DNA solutions containing these psoralen derivatives show only a practically negligible absorption at 300–380 nm (traces b and c, respectively).

These results allow us to confirm that the condensation of a fourth cyclopentane ring at the level of 3,4 pyrone side double bond ensures the intercalation process and that also for the cyclopentenepsoralen moiety, as already stated for benzo- and tetrahydrobenzo-psoralens, the presence of a dimethylamminopropoxy side chain, protonable at physiological pH, confers a significant improvement in the DNA binding properties.[9,10]

2.6. Photobinding to DNA

The capacity of the intercalated cyclopentenepsoralen moiety to photoadd covalently to DNA bases following UVA irradiation was estimated by evaluating photoadduct formation. In particular, the irradiation at 365 nm of a DNA solution in the presence of compounds **3**–**5**, followed by precipitation and acid hydrolysis, as reported in Section 4, allowed us to identify a photoproduct characterised by a violet fluorescence upon 365 nm.

The fluorescent compound obtained from the photoreaction between **5** and the macromolecule was isolated and then characterised by means of spectroscopic techniques. In particular, the UV absorption spectrum shows the disappearance of the band around 300 nm, peculiar for the psoralen chromophore, and the appearance of a band at 330 nm (Fig. 2, line a). Both the strong violet fluorescence and the presence of a band at 330 nm in the UV spectrum are indicative of 4′,5′-cycloadducts between **5** and a pyrimidine base, as already demonstrated for other psoralen–DNA photoproducts.[21] Further evidence for this assumption derives from photoreversal experiments. In detail, it is known that the irradiation at 254 nm of the C_4-cycloadducts induces breakage, giving the parent compound and the DNA base. In Figure 2 are shown the UV spectra of the ethanol solution of the photoproduct before (line a) and after increasing times of irradiation (lines b–e). It is possible to note that, as the period of irradiation increases, there is a gradual increase in the absorption band at 300 nm which occurs concurrently with a decrease of the peak at 330 nm. In particular, after 120 min (line e) a spectrum practically superimposable to that of **5** was obtained. Nevertheless, the confirmation of the structure of the isolated photoproduct was attained from NMR analysis. ^{1}H NMR (DMSO-d_6): δ 1.45 (s, 3H, 4′-Me), 1.47 (s, 3H, 5-Me_T), 1.79 (m, 2H, –CH_2–), 2.21 (s, 6H, $N(CH_3)_2$), 2.73 (m, 2H, –CH_2–N), 4.35 (m, 2H, –CH_2–; d, 1H, 6-CH_T, J = 5.5 Hz), 5.13 (d, 1H, 5′-CH, J = 5.5 Hz), 6.90 (s, 1H, 5-CH), 7.73 (br, 1H, CONH), 9.64 (br, 1H, CONHCO). It is possible to note that the signals corresponding to the proton in position 5′

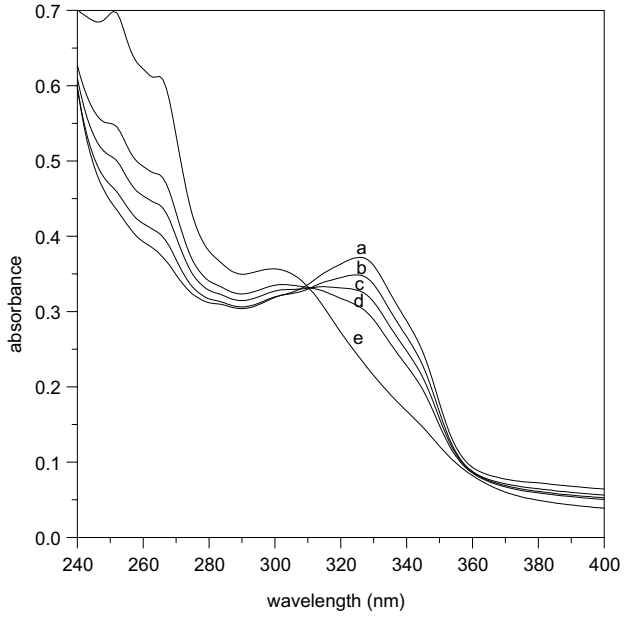

Figure 2. UV absorption spectra of an ethanol solution of furan cycloadduct obtained from DNA and **5** before (line a) and after irradiation at 254 nm for 5, 15, 30 and 120 min (lines b–e, respectively).

of compound **5** (7.88 ppm) and the proton 6 of the thymine (7.24 ppm) shifted to higher fields in the photoadduct (5.13 and 4.35 ppm respectively), which is evidence that the molecular system is no longer that of an aromatic. Besides, both protons presented a coupling between them of 5.5 Hz and lost the allylic coupling with the corresponding methyl groups. In the same way, the signals of the two methyl groups of the photoproduct are shifted to a higher field than in the corresponding precursors due to them no longer being allylic protons. The methyl group in position 4′ of compound **5** (2.23 ppm) and the methyl group of thymine (1.70 ppm) shift to 1.45 and 1.47 ppm in the photoadduct respectively. This spectral data confirms the cycloaddition [2+2] between the double bond 4′,5′ of compound **5** and the double bond 5,6 of the thymine.

Regarding compounds **3** and **4**, the photoproduct corresponding to the fluorescent band showed only a very weak spectral signal in the UV absorption region (spectra not shown), thus indicating under our experimental conditions, a negligible ability to photoreact with the macromolecule. These data are considered to be in accordance with the data shown in Table 2 indicating the inability of both **3** and **4** to exert detectable antiproliferative effect on cells upon UVA irradiation.

2.7. Cross-linking

The occurrence of cross-links between two complementary strands of DNA constitutes cellular damage significant enough to trigger the antiproliferative effect. It was widely demonstrated that the 4′,5′ monoadduct can photoreact following UVA irradiation (365 nm) at the level of 3,4 pyrone side double bond giving rise to this molecular event. Nevertheless, in previous studies devoted to tetracyclic psoralen derivatives it was possible to show that both the chemical structure and the side of the condensation of the fourth ring can strongly influence this ability. In particular, the condensation of a benzene ring compromises the photoreactive capacity of the double bond involved in the condensation, while neither a cyclohexane nor a cyclopentane seem to prevent the covalent photocycloaddition. Furthermore, pyrone side tetracyclic psoralen derivatives appear to be able to induce cross-links less efficaciously with respect to the furan side congeners.[10–12] In Figure 3 the cross-linking ability of **3**–**5** is shown in comparison with the drug 8-MOP, as a function of irradiation time. The considered cyclopentenepsoralen derivatives show a very different behaviour: **4** appears to be unable to give rise to interstrand cross-links, compound **3** shows a weak ability to induce this molecular damage, while the derivative carrying the dimethylaminopropoxy side chain (compound **5**) exerts a cross-link capacity comparable to that scored for the reference drug. These results can be considered to be in accordance with the low complexation ability (see Fig. 1) and the consequent low photoaddition capacity of **3** and **4** with respect to **5**. Otherwise, despite the comparable ability to induce interstrand cross-links, the antiproliferative effect exerted by **5** appears significantly higher with respect to that induced by 8-MOP (see Table 2). These results suggest that notwithstanding the undoubted cytotoxic outcome of the diadduct formation between DNA strands, other photobiological consequences could play a crucial role in the photoantiproliferative effect.

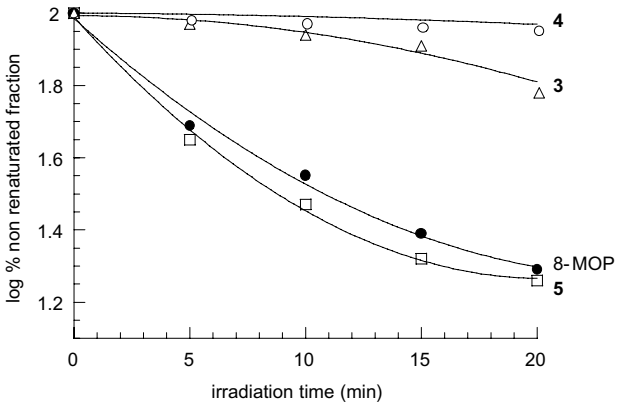

Figure 3. Cross-linking of compounds **3**–**5** and 8-MOP to double-stranded DNA (nucleotide-drug ratio = 75) as a function of irradiation time.

2.8. Back-projection study

A forward towards future modifications of compound **5** to improve its activity could be derived from the back-projection analysis of the compound, using the approach reported elsewhere.[20] As depicted in Figure 4, the furocoumarin framework accounts for 65% of the activity of compound **5**, a result pointing to this nucleus as being the pharmacophore. Interestingly, the same analysis applied to a tetrahydrobenzo-psoralen derivative indicates the contribution of the psoralen chromophore to the activity of the molecule to be 28.5%.[20] In this connection, it is noteworthy that the photoantiproliferative activity evaluated for the tetrahydrobenzopsoralen derivative appears to be from 3 to 6 times lower than that of **5**, depending on the cell line taken into account.[9]

The 3,4-propylene bridge accounts for 11% of the activity, which could be explained by taking into consideration that this feature extends the planar system allowing a better intercalating action of the chemical between the DNA bases. The high contribution predicted for the $-N(CH_3)_2$ group justifies its introduction, probably by increasing the interaction with DNA and the

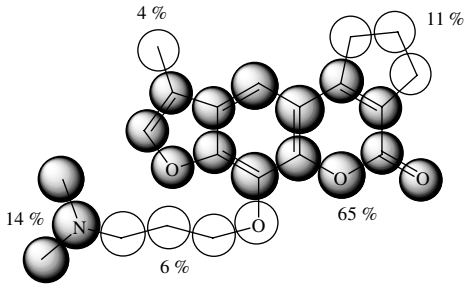

Figure 4. Back-projection for compound **5**.

biodisponibility of the molecule. Finally, the relatively low contribution for the –(CH_2)– chain and the CH_3 group clearly indicates that these moieties may be the object of future synthesising strategies.

3. Conclusions

QSAR directed synthesis of 3,4-cyclopentenepsoralens **3**–**5** was performed. The evaluation of photoantiproliferative activity on human tumour cell lines appears to be in agreement with the posterior probability theoretically calculated. The study of the photobiological properties of the new compounds highlights the interesting behaviour of the derivative **5** characterised by the presence of the dimethylamminopropoxy side chain. Finally, the back-projection analysis of **5** makes it possible to demonstrate the contribution of the various structural moieties to the antiproliferative activity, with a view to the development of rationally conceived new photochemotherapeutic drugs endowed with improved photobiological properties.

4. Experimental

4.1. QSAR methodology

To predict in silico the posterior probability of novel compounds, the following equation was used:[20]

$$\begin{aligned} \mathrm{ACA} &= 3.03\,{}^{\mathrm{SR}}\pi_0 - 49.5\,{}^{\mathrm{SR}}\pi_1 + 126.6\,{}^{\mathrm{SR}}\pi_2 \\ &\quad - 165.8\,{}^{\mathrm{SR}}\pi_4 + 215.6\,{}^{\mathrm{SR}}\pi_8 - 128.2\,{}^{\mathrm{SR}}\pi_{10} - 6.6 \\ N &= 681,\ \ \lambda = 0.44,\ \ F = 141.31, \\ D^2 &= 5.8,\ \ p < 0.00 \end{aligned} \tag{1}$$

where, ACA is 'anticancer activity' and the ${}^{\mathrm{SR}}\pi_k$ are molecular descriptors codifying the distribution of electrons in the molecule. The calculation of the ${}^{\mathrm{SR}}\pi_k$ values for a drug has been explained in detail elsewhere.[16–20] The present procedure considers the external electron layers of any atom core in the molecule (valence shell) as states of a Markov Chain (MC). The method uses the matrix ${}^1\Pi$, which has the elements ${}^1p_{ij}$. ${}^1\Pi$ is built as a square table of order n, where n represents the number of atoms in the molecule. The elements (${}^1p_{ij}$) of ${}^1\Pi$ represent the probabilities with which electrons move from atom i to j:

$${}^1p_{ij} = \frac{\chi_j}{\sum_{k=1}^{\delta+1}\chi_k} \tag{2}$$

where, χ_j is Pauling's electronegativity for the atom aj, which binds to the atom ai. In this equation δ is the number of atoms, which compete with ai by its own electrons (atoms bound to ai), the number 1 accounts for the atom ai per se. The use of the MC theory also allows calculation of the probabilities ${}^kp_{ij}$ with which electrons move between nonbonded atoms throughout the molecular backbone. These probabilities are the elements of the matrices ${}^k\Pi$, which are the natural powers of ${}^1\Pi$, it means that ${}^k\Pi = ({}^1\Pi)^k$.[16–20] The different ${}^{\mathrm{SR}}\pi_k$ can be calculated afterwards by summing up the probabilities on the main diagonal of the ${}^k\Pi$ as molecular descriptors.

$${}^{\mathrm{SR}}\pi_k(\omega) = \sum_{i=1}^{g} {}^kp_{ii} \tag{3}$$

In classical Markov theory, these numbers are the probabilities with which the system returns to the initial state. In the present context, they are the probabilities with which electrons return to the atoms at different times after delocalisation to other atoms in the molecule. That is to say, these numbers encode the distribution of electrons on the molecule.[16–20]

In detail, the model used in this work was derived from a data set containing a large number of compounds ($N = 681$). The values of the different statistical parameters (λ = Wilks' statistic, F = Fisher's ratio, D^2 = square Mahalanobis distance, and $p = p$-level) demonstrate the high significance of the model.

The Wilks' statistic for overall discrimination should take values in the range from 0 (perfect discrimination) to 1 (no discrimination). Comparison between Mahalanobis distance (D) and Fisher ratio (F) allows us to check the hypothesis of separation of groups with a probability of error (p-level) of $p < 0.05$. This model correctly classified 90.5% of the compounds in the training series, that is, 65 misclassifications in 681 cases, while in the predicting series there were 39 errors in 280 cases, that is, 86.1% correct classification. More specifically, the model correctly classified 90.2% of anticancer compounds in the training series and 84.5% of these compounds in the predicting series. The classification results and the names of each anticancer compound used in both training and predicting series were published elsewhere.[20]

4.2. Chemistry

Melting points were determined in a Reichert Kofler thermopan or in capillary tubes in a Büchi 510 apparatus, and are uncorrected. IR spectra were recorded in a Perkin–Elmer 1640FT spectrometer (KBr disks, ν in cm^{-1}). ^1H and ^{13}C NMR spectra were recorded in a Bruker AMX spectrometer at 300 and 75.47 MHz, respectively, using TMS as internal standard (chemical shifts in δ values, J in Hz). Mass spectra were obtained using a Hewlett–Packard 5988A spectrometer. Elemental analyses were performed on a Perkin–Elmer 240B microanalyser and were within ± 0.4% of calculated values in all cases. Silica gel (Merck 60, 230–400 mesh) was used for flash chromatography (FC). Analytical TLC was performed on plates precoated with silica gel (Merck 60 F_{254}, 0.25 mm).

4.2.1. 3,4-Cyclopenten-7-hydroxy-8-methoxycoumarin (1). A mixture of 2-methoxyresorcinol (10.0 g, 71.36 mmol), 12 M H_2SO_4 (120 mL) and ethyl 2-oxocyclopentanecarboxylate (13.37 g, 85.63 mmol) was stir-

red for 15 h at room temperature and then poured into ice water (100 mL) and the precipitate was recovered by filtration and washed with water. The solid residue was purified by FC with 7:3–4:6 hexane/ethyl acetate as eluent, which gave pure **1** (15.01 g, 91%): mp 192–194 °C (white solid). IR: 3350, 2931, 1691, 1601, 1385, 1070, 805. ^{1}H NMR ($CDCl_3$): 2.19 (m, 2H, CH_2–CH_2–CH_2), 2.90 (t, J = 7.5, 2H, CH_2 in C-3), 3.03 (t, J = 7.6, 2H, CH_2 in C-4), 4.10 (s, 3H, CH_3O), 6.32 (br s, 1H, OH), 6.90 (d, J = 8.5, 1H, H6), 7.08 (d, J = 8.5, 1H, H5). ^{13}C NMR ($CDCl_3$): 22.86 ($CH_2CH_2CH_2$), 30.84 (CH_2 in C-4), 32.68 (CH_2 in C-3), 62.15 (MeO), 112.05 (C-6), 113.53, 120.40 (C-5), 124.43, 134.16, 147.52, 151.52, 157.33 (C-4), 160.05 (C-2). MS *m*/*z* (%): 232 (M^+, 100), 217 (10), 204 (23), 189 (13), 161 (4), 115 (13). Anal. ($C_{13}H_{12}O_4$) C, H.

4.2.2. 7-Acetonyloxy-3,4-cyclopenten-8-methoxycoumarin (2). A mixture of hydroxycoumarin **1** (14.48 g, 62.35 mmol), chloroacetone (10.03 mL, 124.70 mmol) and K_2CO_3 (17.23 g, 124.70 mmol) in dry acetone (300 mL) was refluxed for 24 h at room temperature. The mixture was cooled, the precipitate collected, and the solvent evaporated under reduced pressure. The residue was purified by FC using 7:3–4:6 hexane/ethyl acetate as eluent, which gave pure **2** (13.78 g, 77%): mp 150–152 °C (white solid). IR: 2950, 1707, 1611, 1298, 1107, 80. ^{1}H NMR ($CDCl_3$): 2.20 (m, 2H, $CH_2CH_2CH_2$), 2.31 (s, 3H, CH_3CO), 2.90 (t, J = 7.5, 2H, CH_2 in C-3), 3.03 (t, J = 7.6, 2H, CH_2 in C-4), 4.02 (s, 3H, CH_3O), 4.70 (s, 2H, CH_2O), 6.74 (d, J = 8.7, 1H, H6), 7.10 (d, J = 8.7, 1H, H5). ^{13}C NMR ($CDCl_3$): 22.46 ($CH_2CH_2CH_2$), 26.53 (CH_3CO), 30.53 (CH_2 in C-4), 32.18 (CH_2 in C-3), 61.63 (CH_3O), 74.18 (CH_2O), 110.28 (C-6), 114.73, 119.58 (C-5), 125.62, 136.96, 148.41, 152.85, 156.14, 159.61 (C-2), 204.52 ($COCH_3$). MS *m*/*z* (%): 289 ($[M+1]^+$, 37), 288 (M^+, 100), 245 (96), 215 (14), 200 (44). Anal. ($C_{16}H_{16}O_5$) C, H.

4.2.3. 3,4-Cyclopenten-4′-methyl-8-methoxyfuro[3,2-*g*]-coumarin (3). Oxo-ether **2** (13.05 g, 45.26 mmol) was refluxed in 1 M NaOH (280 mL) for 24 h. The mixture was cooled and acidified with 2 M HCl, and the precipitate formed was collected, washed with water, and purified by FC with 9:1–1:1 hexane/ethyl acetate as eluent, to give pure **3** (10.2 g, 83%): mp 216–217 °C. IR: 3104, 2931, 1718, 1618, 1587, 1092, 812. ^{1}H NMR ($CDCl_3$): 2.21 (m, 2H, $CH_2CH_2CH_2$), 2.24 (d, J = 1.3, 3H, CH_3 in C-4′), 2.89 (t, J = 7.5, 2H, CH_2 in C-3), 3.09 (t, J = 7.7, 2H, CH_2 in C-4), 4.25 (s, 3H, CH_3O), 7.09 (s, 1H, H5), 7.43 (d, J = 1.3,1H, H5′). ^{13}C NMR ($CDCl_3$): 8.43 (Me–C4′), 22.95 ($CH_2CH_2CH_2$), 31.27 (CH_2 in C-4), 33.20 (CH_2 in C-3), 61.85 (CH_3O), 108.39 (C-5), 116.50, 116.54, 126.21, 128.10, 133.14, 143.27 (C-5′), 143.77, 147.78, 157.22, 160.43 (C-2). MS *m*/*z* (%): 271 ($[M+1]^+$, 17), 270 (M^+, 100), 242 (84), 199 (13), 141 (10), 128 (19). Anal. ($C_{16}H_{14}O_4$) C, H.

4.2.4. 3,4-Cyclopenten-8-hydroxy-4′-methylfuro[3,2-*g*]-coumarin (4). A mixture of $AlCl_3$ (591.0 mg, 4.43 mmol) and anhydrous CH_2Cl_2 (20 mL) was stirred for 2 h at room temperature. Compound **3** (400 mg, 1.47 mmol) in anhydrous CH_2Cl_2 (20 mL) was added and the mixture stirred for another 3 h. The reaction was then acidified with 1 M HCl and extracted with CH_2Cl_2 (50 mL × 3). The extract was dried (Na_2SO_4) and the solvent evaporated under reduced pressure to leave a residue which was purified by FC using 1–5% MeOH/CH_2Cl_2 as eluent to give pure **4** (328 mg, 87%): mp 329–332 °C (yellow solid). IR: 3311, 2922, 1702, 1593, 1271, 1069, 842. ^{1}H NMR (DMSO-d_6): 2.15 (m, 2H, $CH_2CH_2CH_2$), 2.23 (d, J = 1.0, 3H, CH_3 in C-4′), 2.79 (t, J = 7.4, 2H, CH_2 in C-3), 3.15 (t, J = 7.6, 2H, CH_2 in C-4), 7.25 (s, 1H, H5), 7.83 (dd, J = 1.0, 1H, H5′), 10.49 (br s, 1H, OH). ^{13}C NMR (DMSO-d_6): 7.49 (CH_3 in C-4′), 21.87 ($CH_2CH_2CH_2$), 30.19 (CH_2 in C-4), 32.13 (CH_2 in C-3), 105.09 (C-5), 115.30, 115.56, 124.34, 126.48, 129.89, 140.00, 143.25 (C-5′), 144.90, 157.16, 159.00 (C-2). MS *m*/*z* (%): 257 ($[M+1]^+$, 14), 256 (M^+, 88), 228 (100), 201 (21), 171 (4), 128 (12). Anal. ($C_{15}H_{12}O_4$) C, H.

4.2.5. 3,4-Cyclopenten-8-(3-dimethylaminopropoxy)-4′-methylfuro[3,2-*g*]coumarin (5). A mixture of the phenol **4** (200 mg, 0.78 mmol), 3-chloro-*N*,*N*-dimethylpropylamine hydrochloride (148.0 mg, 0.93 mmol), 60% NaH (56 mg, 2.34 mmol), NaI (140.0 mg, 0.93 mmol) and dimethylformamide (40 mL) was heated for 12 h at 100 °C. After cooling, the precipitate was filtered out and the filtrate concentrated under reduced pressure. The residue was purified by FC with 5:95 CH_2Cl_2/MeOH as eluent, to give pure **5** (169 mg, 64%): mp 107–108 °C (yellow solid). IR: 3424, 2947, 1711, 1589, 1457, 1188, 751. ^{1}H NMR (DMSO-d_6): 1.86 (m, 2H, CH_2CH_2O), 2.12 (s, 6H, $(CH_3)_2N$), 2.14 (m, 2H, $CH_2CH_2CH_2$), 2.23 (d, J = 1.3, 3H, CH_3 in C-4'), 2.44 (t, J = 7.0, 2H, CH_2N), 2.78 (t, J = 7.6, 2H, CH_2 in C-3), 3.15 (t, J = 7.6, 2H, CH_2 in C-4), 4.41 (t, J = 6.4, 2H, CH_2O), 7.45 (s, 1H, H5), 7.88 (d, J = 1.3, 1H, H5′). ^{13}C NMR (DMSO-d_6): 7.36 (CH_3 in C-4′), 21.74 ($CH_2CH_2CH_2$), 27.66 (CH_2CH_2O), 30.19 (CH_2 in C-4), 32.06 (CH_2 in C-3), 45.10 (CH_3N), 55.33 (CH_2N), 71.58 (CH_2O), 108.72 (C-5), 115.34, 15.54, 124.54, 126.89, 130.75, 142.88, 143.51 (C5′), 146.83, 156.70, 158.63 (C2). MS *m*/*z* (%): 341 (M+, 11), 312 (3), 256 (22), 228 (20), 178 (34), 58 (100). Anal. ($C_{20}H_{23}NO_4$) C, H, N.

4.3. Cell cultures

HeLa and HL-60 cells were grown in Nutrient Mixture F-12 [HAM] (Sigma Chemical Co.) supplemented with 10% heat-inactivated foetal calf serum (Biological Industries) and RPMI 1640 (Sigma Chemical Co.) supplemented with 15% heat-inactivated foetal calf serum (Biological Industries), respectively. Penicillin (100 U/mL), streptomycin (100 μg/mL) and amphotericin B (0.25 μg/mL) (Sigma Chemical Co.) were added to both media. The cells were cultured at 37 °C in a moist atmosphere of 5% carbon dioxide in air.

4.4. Irradiation procedure

Irradiations were performed by means of Philips HPW 125 lamps equipped with a Philips filter emitting over 90% at 365 nm. Irradiation intensity was checked on a

UV-X radiometer (Ultraviolet Products Inc., Cambridge, UK) for each experimental procedure.

4.5. Inhibition growth assays

HeLa cells (10^5) were seeded into each well of a 24-well cell culture plate. After incubation for 24 h, the medium was replaced with an equal volume of Dulbecco's modified Eagle medium (DMEM, Sigma Chemical Co.) without phenol red, and various concentrations of the test agent were added. One hour later the cells were irradiated with a UVA dose of 0.793 J cm^{-2}. After irradiation, the medium containing the compounds was removed, and the cells were incubated in complete F-12 medium for 24 h.

HL-60 cells (10^5) were seeded into each well of a 24-well cell culture plate. After incubation for 24 h, various concentrations of the test agents were added in complete medium. The cells were kept in the dark for 1 h, irradiated with a UVA dose of 0.793 J cm^{-2} and then incubated for a further 24 h.

In the case of the experiments carried out in the dark both HeLa and HL-60 were seeded (10^5) and incubated for 24 h. Then, the test agent was added and the cells were incubated for further 24 h.

A trypan blue assay was performed to determine cell viability. Cytotoxicity data were expressed as IC_{50} values, that is, the concentrations of the test agent inducing 50% reduction in cell numbers compared with control cultures.

4.6. Skin phototoxicity

Skin phototoxicity was tested on depilated albino guinea pigs (outbred Dunkin–Hartley strain), as previously reported.[22] An ethanol solution of each new compound was applied topically to the skin up to 50 μg/cm^2. For 8-MOP the concentration used was 10 μg/cm^2. The animals were then kept in the dark for 45 min and the treated skin was irradiated with 20 kJ m^{-2} of UVA; erythema was scored after 48 h.

4.7. Nucleic acid

Salmon testes DNA was purchased from Sigma Chemical Company (Cat. D-1626). Its hypochromicity, determined according to Marmur and Doty,[23] was over 35%. The DNA concentration was determined using extinction coefficient 6600 M^{-1} cm^{-1} at 260 nm.

4.8. Linear flow dichroism

Linear dichroism (LD) measurements were performed on a Jasco J500A circular dichroism spectropolarimeter converted for LD and equipped with an IBM PC and a Jasco J interface.

Linear dichroism is defined as

$$LD_{(\lambda)} = A_{\parallel(\lambda)} - A_{\perp(\lambda)}$$

where $A_{\parallel}$ and $A_{\perp}$ correspond to the absorbances of the sample when polarised light is oriented parallel or perpendicular to the flow direction, respectively. The orientation is produced by a device designed by Wada and Kozawa[24] at a shear gradient of 500–700 rpm and each spectrum was accumulated four times.

A solution of salmon testes DNA (1.5×10^{-3} M) in ETN buffer (containing 10 mM TRIS, 10 mM NaCl and 1 mM EDTA, pH = 7) was used. Spectra were recorded at 25 °C at [drug]/[DNA] = 0, 0.02, 0.04 and 0.08.

4.9. Preparation of adducts

Volumes of concentrated solutions of the examined compound were added to salmon testes DNA in ETN solution (1.5×10^{-3} M) to achieve a DNA/compound ratio of about 80. The mixture was irradiated in a glass dish with four Philips HPW 125 lamps (6.58 mW cm^{-2}), arranged two above and two below the dish, at a distance of 7 cm, for 120 min at room temperature. After irradiation the DNA was precipitated with NaCl (up to 1 M concentration) and cool ethanol (2 vol), the precipitated DNA was collected, washed with 80% ethanol, dried and then dissolved in a measured volume of buffer. The final solution was made 0.5 N with HCl, heated at 100 °C for 2 h, neutralised with NaOH and extracted exhaustively with $CHCl_3$. After this procedure the organic layers were collected, dried under high vacuum and dissolved in ethanol. The adduct was separated on TLC plates eluted with $CHCl_3$/ethanol 1:1. NMR analysis of the adduct was performed on a Bruker 300 spectrometer.

4.10. Photoreversal of adducts

Ethanol solution of the adduct was irradiated in quartz cuvettes with a mineral lamp (254 nm). The photosplitting reaction was followed spectrophotometrically. UV spectra were recorded on a Perkin–Elmer model Lambda 40 spectrometer.

4.11. Evaluation of interstrand cross-links in vitro

Evaluation of cross-links was carried out by measuring the renaturation capacity of cross-linked DNA after thermal denaturation. Aliquots of solution of DNA and examined compound [DNA]/[drug] = 75 were introduced into calibrated glass tubes, immersed in a thermostatically controlled bath, and then irradiated for various periods of time. After irradiation the samples were thermally denatured (95 °C for 15 min) and quickly cooled in ice. The renaturation capacity of DNA, due to cross-link formation, was investigated by recording absorbance at 260 nm. Data were expressed in terms of log% of nonrenaturated fraction of irradiated compound–DNA complex relative to irradiated DNA, as suggested by Blais et al.[25]

4.12. Back-projection methodology

This analysis makes it possible to calculate the contribution of the different atoms in the molecule to the phar-

macological activity. First, the $^{SR}\pi_k$ values for each atom in the molecule are calculated and afterwards they are evaluated in the model.[20] All values are normalised in 0–100 scale.

References and notes

1. Lowe, N. J.; Chizhevsky, V.; Gabriel, H. *Clin. Dermatol.* **1997**, *15*, 745.
2. Bethea, D.; Fullmer, B.; Syed, S.; Seltzer, G.; Tiano, J.; Rischko, C.; Gillespie, L.; Brown, D.; Gasparro, F. P. *J. Dermatol. Sci.* **1999**, *19*, 78.
3. Edelson, R. L. *Ann. N.Y. Acad. Sci.* **1991**, *636*, 154.
4. Oliven, A.; Shechter, Y. *Blood Rev.* **2001**, *15*, 103.
5. McNeely, W.; Goa, K. L. *Drugs* **1998**, *56*, 667.
6. Stern, R. S. *J. Am. Acad. Dermatol.* **2001**, *44*, 755.
7. Wang, S. Q.; Setlow, R.; Berwick, M.; Polsky, D.; Marghoob, A. A.; Kopf, A. W.; Bart, R. S. *J. Am. Acad. Dermatol.* **2001**, *44*, 837.
8. Hearst, J. E. *Chem. Res. Toxicol.* **1989**, *2*, 69.
9. DallaVia, L.; Gia, O.; Marciani Magno, S.; Santana, L.; Teijeira, M.; Uriarte, E. *J. Med. Chem.* **1999**, *42*, 4405.
10. DallaVia, L.; Uriarte, E.; Quezada, E.; Dolmella, A.; Ferlin, M. G.; Gia, O. *J. Med. Chem.* **2003**, *46*, 3800.
11. DallaVia, L.; Gia, O.; Viola, G.; Bertoloni, G.; Santana, L.; Uriarte, E. *Farmaco* **1998**, *53*, 638.
12. Dalla Via, L.; Uriarte, E.; Santana, L.; Marciani Magno, S.; Gia, O. *Arkivoc* **2004**(V), 131.
13. Kubinyi, H.; Taylor, J.; Ramdsen, C. In *Comprehensive Medicinal Chemistry*; C., Hansch, Ed.; Pergamon, 1990; Vol. 4, pp 589–643.
14. Estrada, E.; Uriarte, E. *Curr. Med. Chem.* **2001**, *8*, 1573.
15. Stieflf, N.; Baumann, K. *J. Med. Chem.* **2003**, *46*, 1390.
16. Gonzalez, D. H.; Olazabal, E.; Castanedo, N.; Hernandez, I.; Morales, A.; Serrano, H.; Gonzalez, J.; Ramos, R. *J. Mol. Mod.* **2002**, *8*, 237.
17. Gonzalez, D. H.; Hernandez, I.; Uriarte, E.; Santana, L. *Comput. Biol. Chem.* **2003**, *27*, 217.
18. Gonzalez, D. H.; Marrero, Y.; Hernandez, I.; Bastida, I.; Tenorio, I.; Nasco, O.; Uriarte, E.; Castanedo, N.; Cabrera, M.; Aguila, E.; Marrero, O.; Morales, A.; Perez, M. *Chem. Res. Toxicol.* **2003**, *16*, 1318.
19. Gonzalez, D. H.; DeArmas, R. R.; Molina, R. *Bioinformatics* **2003**, *19*, 2079.
20. Gonzalez, D. H.; Gia, O.; Uriarte, E.; Hernadez, I.; Ramos, R.; Chaviano, M.; Seijo, S.; Castillo, J. A.; Morales, L.; Santana, L.; Akpaloo, D.; Molina, E.; Cruz, M.; Torres, L. A.; Cabrera, M. A. *J. Mol. Mod.* **2003**, *9*, 395.
21. Caffieri, S.; Dall'Acqua, F. *Photochem. Photobiol.* **1987**, *45*, 13.
22. Gia, O.; Anselmo, A.; Conconi, M. T.; Antonello, C.; Uriarte, E.; Caffieri, S. *J. Med. Chem.* **1996**, *39*, 4489.
23. Marmur, J.; Doty, P. *J. Mol. Biol.* **1962**, *5*, 109.
24. Wada, A.; Kozawa, S. *J. Polym. Sci.: Part A* **1964**, *2*, 853.
25. Blais, J.; Vigny, P.; Moron, J.; Bisagni, E. *Photochem. Photobiol.* **1984**, *39*, 145.